Adsorption (2014) 20:737–746
DOI 10.1007/s10450-014-9617-9

How do the HSDM and Boyd's model compare for estimating intraparticle diffusion coefficients in adsorption processes

Rui M. C. Viegas · Margarida Campinas · Helena Costa · Maria João Rosa

Received: 22 November 2013 / Revised: 16 May 2014 / Accepted: 16 June 2014 / Published online: 25 June 2014

Abstract Adsorption kinetics is a key-issue for a successful activated carbon selection and design of the treatment system. Crucial predictive aspects are the determination of the diffusion coefficients and the establishment of the controlling adsorption step. Several kinetic models have been developed and two of the most frequently used, the homogeneous surface diffusion model (HSDM) and the Boyd's model, were applied to microcystins, and particularly MC-LR adsorption. Different initial MC-LR concentrations and carbons (particle diameter, porosity), yielding diverse Biot numbers (Bi), were tested. The model outcomes were compared, namely the Boyd's effective intraparticle diffusion coefficient (D_i) with the HSDM surface diffusion coefficient (D_s), as well as the Bi and Boyd's criteria to establish the controlling adsorption step, which constitute a novel approach. Very good HSDM fittings were achieved with a constant diffusion model (D_s independent of MC-LR surface concentration). D_i was similar to D_s whenever Boyd plots intercepted the origin. The Biot limit above which it may be considered that intraparticle diffusion is the rate limiting step depended on the carbon. A lower limit was observed for smaller carbons.

Keywords Adsorption kinetic models · HSDM · Boyd model · Intraparticle diffusion coefficient · Microcystins

R. M. C. Viegas (✉) · M. Campinas · H. Costa · M. J. Rosa
Urban Water Division, Hydraulics and Environment Department, LNEC – National Civil Engineering Laboratory, Av. Brasil 101, 1700-066 Lisbon, Portugal
e-mail: rviegas@lnec.pt

Abbreviations

HPLC	High-performance liquid chromatography
HSDM	Homogeneous surface diffusion model
MC–LR	Microcystin-LR
NOM	Natural organic matter
PAC	Powdered activated carbon
PLR	Piecewise linear regression
SPE	Solid phase extraction
SSE	Sum of square errors

Variables

B	Boyd number (-)
Bi	Biot number (-)
C_0	Initial liquid-phase concentration (M/L^3)
C_b (t)	Bulk liquid phase concentration (M/L^3)
C_s (t)	Liquid phase concentration at solid–liquid interface (M/L^3)
d_p	Adsorbate particle diameter (L)
D_s	Surface diffusion coefficient (L^2/T)
D_i	Effective intraparticle diffusion coefficient (L^2/T)
F(t)	Fractional attainment of equilibrium (-)
K_F	Freundlich isotherm capacity constant (units in Table 4)
k_f	External mass transfer coefficient (L/T)
M	Total mass of carbon (M)
n	Freundlich isotherm constant
q	Solid-phase concentration (M/M)
q_e	Solid-phase concentration in equilibrium (M/M)
q(r, t)	Solid phase concentration (M/M)
q_{avg}	Average solid phase concentration (M/M)
q_s	Solid phase concentration at solid–liquid interface (M/M)
q_0	Initial solid phase concentration (M/M)
r	Radial coordinate (L)
R	Radius of adsorbent particle (L)

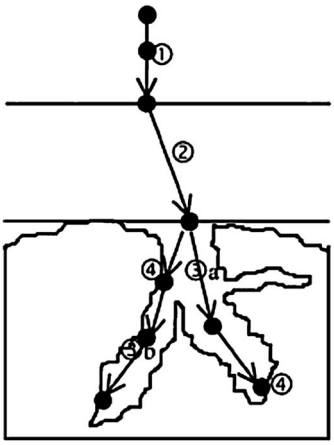

Position	Phenomenon	Coefficient
Bulk of solution	① Diffusion/Convection	Fast
Outer layer	② External Mass Transfer	k_f
GAC particle	③a Porous Diffusion	D_p
	③b Surface Diffusion	D_s
	④ Adsorption	Instantaneous

Fig. 1 Diffusion mechanisms involved in the adsorption process (Adapted from Baup et al. 2000)

t Time (T)
V Liquid-phase volume (L^3)

Greek symbol
ρ_p Apparent density of particle (M/L^3)

1 Introduction

Episodes of micropollutants are often controlled by powdered activated carbon (PAC) addition in drinking water and wastewater treatment plants due to its practical use and effectiveness. Activated carbons are usually selected based on their adsorption capacity for a specific contaminant (adsorbate) but the solute's rate of removal is also a crucial factor for designing the system. Different adsorbents have different pore structures and different surface chemistries, consequently adsorption rates may be controlled by pore, surface or external film diffusion or by a combination of these transport resistances (Choy et al. 2004).

In the past decades, several mathematical models have been proposed to describe the adsorption kinetic data, which can generally be classified as adsorption reaction models and adsorption diffusion models (Qiu et al. 2009). The latter are always based on three steps (Fig. 1) (Ho and McKay 1998; Baup et al. 2000; Ocampo Pérez et al. 2012):

1. Mass transfer of solute from the bulk solution through the stagnant film surroundings to the particle external surface (external or film mass transport);
2. Mass transfer of solute within the particle (internal or intraparticle diffusion). Intraparticle diffusion may be due to pore volume diffusion (diffusion in the fluid-filled pores), surface diffusion (migration along the pore surface in which an adsorbate hops from one to another available adsorption site in a series of adsorption–desorption reactions) or a combination of both (Zhang et al. 2009);
3. Solute attachment onto the surface of the adsorbent surface site—adsorption.

Step 3, adsorption, is usually very rapid compared to the first two steps, and the overall rate of adsorption is therefore often controlled by the first or the second steps, whichever is slower, or a combination of both (Malash and El-Khaiary 2010). Adsorption reaction models, such as first- and second-order kinetic equations, do not describe individually the above mentioned steps (Qiu et al. 2009; Ocampo-Pérez et al. 2012).When these kinetic models are applied it is normally assumed that the overall rate of adsorption is exclusively controlled by the adsorption rate of the adsorbate on the adsorbent surface, and both intraparticle diffusion and external mass transport can be neglected (Ocampo-Pérez et al. 2012).

Several diffusion models, with different degrees of complexity (Marczewski et al. 2013), have been used over the years. One frequently used is the homogeneous surface diffusion model (HSDM) (Ocampo-Pérez et al. 2013). The HSDM predicts the diffusion of a molecule from the external surface of the adsorbent particle through the pore surface to the adsorption site and assumes that internal mass transfer is only due to surface diffusion and that pore volume diffusion resistance is negligible (Baup et al. 2000). The HSDM has been effectively used to determine the surface diffusion coefficient (D_s) of several solutes and to predict the PAC dosages for full-scale systems (Cook and Newcombe 2008; Zhang et al. 2009).

On the other hand, Boyd's intraparticle diffusion model (Boyd et al. 1947) is currently one of the most widely used models for studying the adsorption mechanisms (Malash

and El-Khaiary 2010). Boyd's model is frequently applied to kinetic data to analyse which is the rate limiting step, intraparticle diffusion or film diffusion, but this model also allows establishing the effective intraparticle diffusion coefficient (D_i).

Until now the application of both models is rather independent, and a comprehensive analysis of how does the Boyd's model compare with the HSDM to estimate the intraparticle diffusion coefficient in adsorption processes is still lacking.

Therefore, the aim of this article is to fill this gap of knowledge and more specifically to assess Boyd's model applicability to estimate the intraparticle diffusion coefficients in adsorption processes. To investigate the importance of external mass transfer compared to intraparticle diffusion both the Biot number (Bi) and Boyd's model criteria were used, the former using the coefficients obtained from the HSDM.

Microcystin-LR (MC-LR) was selected as the target compound since it is an environmental health hazard of chemical interest and increasing concern due to climate change effects. On one hand, MC-LR is hepatotoxic, tumour-promoter and the most commonly occurring cyanotoxins. On the other hand, while the relative size of the target adsorbate compared to natural organic matter (NOM) size distribution and activated carbon porous distribution is a key feature for micropollutant adsorption, MC-LR, with a molar mass of 994 Da (Campinas and Rosa 2006), is larger than most micropollutants studied. Besides, cyanobacterial blooms, and consequently cyanotoxin detection, are often seasonal episodes controlled by PAC addition to drinking water treatment, and surface diffusion models have shown to accurately describe the PAC adsorption kinetics of microcystins (Cook and Newcombe 2008).

Experiments were performed with several MC-LR concentrations and carbons with different particle diameters and MC-LR adsorption capacities, which yielded a range of Biot numbers.

2 Theory

2.1 Boyd's model

Boyd et al. (1947) developed theoretical models for ion-exchange kinetics. The adsorption community found that these kinetic models also applied to adsorption systems and Boyd's diffusion models have since been applied in numerous adsorption studies (Castillejos et al. 2011; El-Khaiary and Malash 2011), mostly to determine the rate-controlling step.

Table 1 Boyd's model equations (Boyd et al. 1947 and Reichenberg 1953)

Equation		
$F = \frac{q}{q_e} = 1 - \frac{6}{\pi^2} \times \sum_{n=1}^{\infty} \frac{1}{n^2} \times e^{-n^2 \times Bt}$	(1)	
$B = \frac{\pi^2 \times D_i}{R^2}$	(2)	
$Bt = -\ln \frac{\pi^2}{6} - \ln (1 - F(t))$	(3)	for $F(t) > 0.85$
$Bt = \left(\sqrt{\pi} - \sqrt{\pi - \frac{\pi^2 F(t)}{3}}\right)^2$	(4)	for $F(t) \leq 0.85$

Following Boyd's model (equations on Table 1; variables defined in the Nomenclature section) diffusion processes were considered, namely particle diffusion and film diffusion. Under conditions where particle diffusion is the sole rate-controlling process, Eq. (1) (in Table 1) holds, where B is given by Eq. (2) (Boyd et al. 1947). The assumptions for these equations are (Reichenberg 1953):

1. F is a mathematical function of Bt and vice versa. The values of Bt may be plotted against the experimental values of t and a straight line (of B slope) passing through the origin should be obtained provided the diffusion coefficient D_i does not vary with F over the range of values involved;
2. For a given value of t, F depends only on D_i/R^2, i.e. F is independent of the concentration of solute ions;
3. B is inversely proportional to the square of the particle radius. For a given value of F, dF/dt and dq/dt are proportional to B, and the rate of exchange will be inversely proportional to the square of the particle radius for all values of F under conditions of particle diffusion.

By applying Fourier transform and then integrating Eq. (1) for $F(t) > 0.85$ and $F(t) \leq 0.85$, Reichenberg (1953) obtained the approximations given by Eq. (3) and Eq. (4), respectively (Table 1).

According to this model, if the intraparticle diffusion is the adsorption rate controlling step then the plot of Bt (calculated by Eq. (3) or Eq. (4)) against time (Boyd plot) produces a straight line that passes through the origin. In this case the Boyd's coefficients may be determined, B by the slope of Bt vs. t and Di by Eq. (2). If the plot is nonlinear or linear but does not pass through the origin, it can then be concluded that the limiting step is the film-diffusion or the chemical reaction (El-Khaiary and Malash 2011; Sharma and Das 2012).

The Boyd's plots often have a multilinear nature and statistical tools coupled with conventional graphical analysis are therefore needed to decide about the number and

Table 2 Basic equations for the HSDM (adapted from Roy et al. 1993)

Equation		Role
$\frac{dC_b}{dt}V = -M\frac{dq_{avg}}{dt}$	(5)	Mass balance for closed batch test
$q_{avg} = \frac{3}{(d_p/2)^3}\int_0^{d_p/2} q(r,t)r^2 dr$	(6)	Average carbon load
$\frac{\partial q}{\partial t} = \frac{D_s}{r^2}\frac{\partial}{\partial r}(r^2\frac{\partial q}{\partial r})$	(7)	Diffusion equation for a spherical particle
$q(r,0) = 0$	(8)	Initial condition
$\frac{\partial q}{\partial r} = 0$ for $r = 0$	(9)	Boundary condition for the centre of the spherical particle
$\rho_p D_s \frac{\partial q}{\partial r} = k_r(C_b - C_s)$	(10)	Boundary condition for continuity of flux at $r = d_p/2$
$q_s = K_F C_s^n$	(11)	Freundlich isotherm for equilibrium at solid–liquid interface

location of breakpoints, minimising the subjectivity of linear segments determined only by visual analysis. The piecewise linear regression (PLR) statistical method was used in a Microsoft Excel™ spread sheet developed by Malash and El-Khaiary (2010).

PLR calculations were performed considering one, two, three and four linear segments. For each case, the regression was estimated, the segmented line produced was graphically assessed and the confidence intervals of the linear segments were checked.

When all estimates made sense and were statistically accepted, the models were compared for the goodness of fit using a statistical F-test based on the extra sum of square errors (SSE). The F-test was derived from hypothesis testing and analysis of variance (ANOVA). This is, the difference between the SSE of the two models being compared were analysed, taking into account the number of data points and the number of parameters in each model. This information was used to calculate a F ratio and a *P* value, obtained from the F distribution, using the Microsoft® Excel™ FDIST function (Malash and El-Khaiary 2010). If the calculated *P* value was less than 0.05, the usually chosen level of significance, one concluded that the complex model fits the data significantly better than the simpler model. Otherwise, the complex model was rejected since there was no statistical evidence that it fits the data better than the simpler model.

2.2 HSDM

The basis of this model was proposed by Mathews and Weber (1976) and included the effect of external mass transfer, unsteady-state surface diffusion in the particle and a nonlinear adsorption isotherm. The assumptions of HSDM are:

1 The adsorbent particle is assumed to be a homogeneous solid sphere in which the adsorbate is transported by surface diffusion;
2 The rate-controlling process is mass transport by film and surface diffusion only;
3 A driving force describes the liquid film resistance to mass transfer at the outer surface of the particle;
4 Instantaneous equilibrium between the carbon particle and the adsorbate occurs at the outer surface of the carbon particle.

The equations describing the HSDM are presented in Table 2 and the variables are defined in the Nomenclature section. There are several methods for solving the HSDM; herein (Roy et al. 1993) approach was used. These authors used the orthogonal collocation method to discretize the partial differential equations of the HSDM to ordinary differential equations with initial conditions, and then applied Laplace transforms to convert the linear ordinary differential equations to algebraic equations (Roy et al. 1993).

2.3 Biot number

Once the external and internal diffusion coefficients are determined for a given adsorption system, or more specifically the mass transfer coefficient (k_f) and the surface diffusion in the particle (D_s) are known, the surface diffusion modified Biot number (Bi) can be estimated from Eq. (12), where C_0 is the initial liquid-phase concentration and q_0 is the solid phase concentration in equilibrium with C_0 (Roy et al. 1993; Erosa et al. 2001).

$$Bi = \frac{k_f \cdot d_p \cdot C_0}{2 \cdot \rho_p \cdot D_s \cdot q_0} \tag{12}$$

The Biot number represents the ratio of the rate of transport across the liquid layer to the rate of diffusion within the particle and provides a criterion for the dominance of external diffusion over surface diffusion. For $Bi \ll 1$ external mass transport resistance is the mass transfer controlling step (Traegner and Suidan 1989; Erosa et al. 2001; Boschi et al. 2011). However, the Bi limit that establishes the dominance of internal diffusion is not

Table 3 Characteristics of the studied activated carbons (adapted from Li et al. (2003), Campinas and Rosa (2006) and Costa (2010))

Characteristics	SA-UF	AQUA	F200
Average particle diameter (μm)	6	21	152.5[a]
pH_{pzc}	9.6	8.4–8.8	7.4 ± 0.8
Total micropore volume (cm^3/g)	0.54	0.36	0.32
Total mesopore volume (cm^3/g)	0.36	0.15	0.14

[a] 125–180 μm are minimum–maximum particle diameters

consensual. While some authors consider Bi ≫ 1 (Erosa et al. 2001; Boschi et al. 2011) others use Bi ≫ 100 (Traegner and Suidan 1989; Roy et al. 1993; Prasad and Srivastava 2009). For the latter, Bi numbers between 1 and 100 indicate that both internal and external mass transfer are important for the adsorption rate.

3 Materials and methods

3.1 Activated carbons

The experimental runs were performed with two PACs, SA-UF (NORIT) and AQUA (Aquasorb BP4 from JACOBI carbons) and one granular activated carbon (GAC), F200 (Calgon Corporation) (Table 3).

Prior to use, F200 GAC (700 μm average diameter) was crushed in a Retsch AS 200 grinder, sequentially sifted through 180 and 125 μm sieves and washed with ultrapure water to remove fines. All carbons were oven dried at 105 °C overnight to remove excess water and stored in a desiccator until use.

3.2 Microcystin-LR

Microcystins (MCs) are cyclic heptapeptides that share a general structure containing five fixed amino acids and two variable L-amino acids, designated as X and Z. The most commonly occurring microcystin contains leucine in position X and arginine in position Z, and is therefore called MC-LR (Sivonen and Jones 1999). In the experimental work conducted with AQUA and F200 carbons pure MC-LR and MC-extract were used, supplied by Jussi Meriluoto (Åbo Akademi University, Finland). The experimental work with SA-UF carbon was performed with a MC-extract from a *Microcystis aeruginosa* laboratory grown culture, as described in Campinas and Rosa (2006). This extract contained four MC variants (MC-LR, MC-LY, MC-LW and MC-LF) detected by high-performance liquid chromatography (HPLC), MC-LR being the dominant (75 % of total microcystins). MC-LR has a molecular weight of 994 Da and molecular dimensions of 1.4–2.6–2.9 nm (Sathishkumar et al. 2010; Zhang et al. 2011) and a net charge of −1 in the pH range tested (5.2–6.7) (Campinas and Rosa 2006).

3.3 Model waters

Kinetic and isotherm tests were carried out with organic and inorganic-free water obtained from a Milli-Q® water purification system (resistance ≥ 18 MΩ/cm). Just before starting the experiments, ultrapure waters were spiked with MC-LR (either pure toxin or extract) to the desired initial MC-LR concentration (μg MC-LR/L when using pure MC or μg $MC\text{-}LR_{eq}$/L when MC-extract was used). The pH of the assayed waters varied between 5.2 and 6.7.

3.4 Analytical methods

Samples were filtered through a Whatman GF/C (1.2 μm; used in AQUA and F200 runs) or GF/F (0.7 μm; in SA-UF runs) filter and the filtrate was passed through a SPE (solid phase extraction) cartridge to extract the toxin(s) for analysis through HPLC with photo-diode array detection (Dionex Summit system). The extraction and analytical procedures used were developed by Meriluoto and Spoof with the adaptations described in Campinas and Rosa (2006).

3.5 Batch adsorption tests

Batch adsorption tests were performed to characterize the adsorption isotherms and kinetics of MC-LR onto AQUA and F200 carbons. The experiments with SA-UF carbon were performed in an earlier study (Campinas et al. 2013) but their description and part of the results are herein included for comparing with the other two carbons. The studied carbons differed in terms of MC-LR adsorption capacity and particle size; accordingly, different experimental conditions were tested with respect to carbon dose and contact time.

Batch equilibrium tests were performed to obtain MC-LR adsorption isotherms. Ultrapure waters spiked with MC-LR were added to 250 mL bottles leaving a 20–30 mL headspace. Activated carbons were added and the bottles were sealed and stirred in an Edmund-Bühler KM–2 orbital shaker (250 rpm, 23 °C) for 65–72 h (the equilibrium time previously determined). Carbon doses tested were 16–60 mg/L for AQUA and F200, and 8–25 mg/L for SA-UF. Toxin concentration was 0.078–0.217 mg $MC\text{-}LR_{eq}$/L, and the mass adsorbed onto carbon was calculated by mass balance.

Identical batch tests were conducted for studying MC-LR adsorption kinetics onto AQUA and F200 carbons and jar-tests (Flocumatic Selecta apparatus) at 200 rpm were

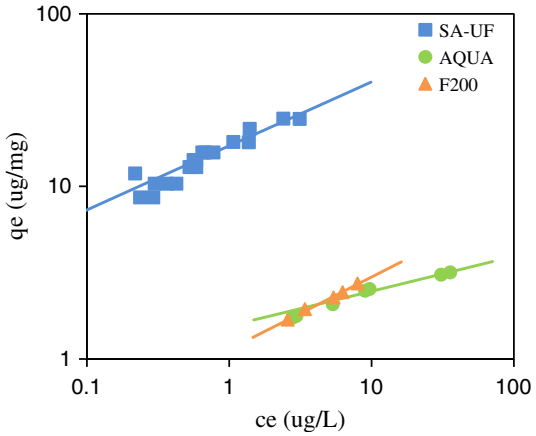

Fig. 2 MC isotherms data and Freundlich model fittings

Table 4 Freundlich parameters for MC-LR adsorption onto SA-UF, AQUA and F200 carbons

Carbon	K_F (μg/mg) $(\mu g/L)^{(1/n)}$	K_F (μmol/mg) $(\mu mol/L)^{(1/n)}$	K_F error (%)	1/n	1/n error (%)	r^2
SA-UF[a]	17	0.22	37	0.37	16	0.934
AQUA	1.6	0.0063	15	0.20	20	0.995
F200	1.1	0.021	33	0.42	16	0.996

[a] data published in Campinas et al. (2013)

performed with SA-UF. Pre-weighted masses of each carbon were soaked overnight in ultrapure water to allow for complete wetting of the pores. Immediately before starting the experiment, a given volume of the model water was added to each batch reactor to make up 80 mL (AQUA and F200) or 500 mL (SA-UF). Samples were taken at predetermined time intervals. Batch tests with AQUA and F200 were conducted with 31 mg/L carbon and a sampling period up to 6 h (AQUA) or 120 h (F200); those with SA-UF were performed with 5 mg/L carbon and samples were taken over a 4 h period. Toxin concentrations of 0.088 mg MC-LR/L (AQUA), 0.079 mg MC-LR/L (F200) and 0.034–0.143 mg $MC\text{-}LR_{eq}$/L (SA-UF) were tested. Identical temperature conditions (21–23 °C) were applied to all batch reactors.

4 Results and discussion

4.1 HSDM results

For the application of the kinetic models a prior characterization of MC-LR adsorption equilibrium was performed. A non-linear Freundlich adsorption model (Eq. 11) was applied to isotherm data, producing the plots and parameters shown in Fig. 2 and Table 4, respectively. Data relative to SA-UF PAC were earlier produced (Campinas et al. 2013) and are herein included for comparison with AQUA and F200 data.

The HSDM (Eq. 5–10) was then applied to the experimental data relative to the adsorption kinetics of MC-LR onto the three studied carbons, SA-UF, AQUA and F200, as illustrated in Fig. 3. For SA-UF (Fig. 3 left), the model fitted simultaneously the three data sets for the three initial concentrations.

HSDM fitting calculations were performed using the software package Scientist™ from MicroMath® (USA). By fitting the model to MC-LR concentrations in the aqueous phase, the two kinetic parameters, k_f and D_s, were obtained (Table 5).

Campinas et al. (2013) found that for SA-UF adsorption k_f and D_s were both independent of the initial MC-LR concentration and k_f showed a minor effect on D_s, a result consistent with other authors' approach, which also considered D_s the main adjustment parameter (Cook and Newcombe 2008) (Table 5).

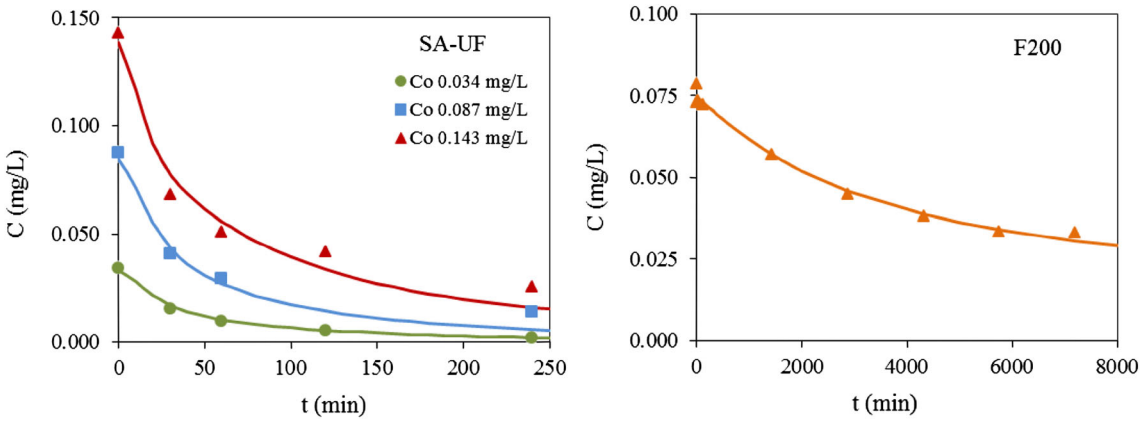

Fig. 3 HSDM fittings for MC-LR adsorption onto SA-UF and F200 carbons

Table 5 HSDM results of MC-LR adsorption onto SA-UF, AQUA and F200 carbons

Carbon	d_p (μm)	C_0 (mg/L)	k_f (m/s)	D_s (m^2/s)	D_s error (%)	r^2	Bi
SA-UF[a]	6	0.034	11×10^{-6}	1.0×10^{-16}	54	0.973	0.7
		0.088					1.3
		0.143					1.8
AQUA	21	0.088	16×10^{-6}	3.4×10^{-16}	47	0.905	21
F200[b]	125	0.079	2.0×10^{-6}	3.1×10^{-16}	15	0.990	16
	152.5			4.7×10^{-16}	16	0.990	13
	180			7.1×10^{-16}	20	0.985	10

[a] data published in Campinas et al. (2013)

[b] minimum, average and maximum particle diameters were considered for this carbon

Table 6 Boyd's model results of MC-LR adsorption onto SA-UF, AQUA and F200 carbons

Carbon	d_p (μm)	C_0 (mg/L)	Bi	Bt vs. t intercept	Bt vs. t crosses origin?	D_i (m^2/s)[c]	D_i error (%)[c]
SA-UF[a]	6	0.034	0.7	–0.08 ± 0.03	No	(1.8×10^{-16})	(4)
		0.087	1.3	–0.08 ± 0.02	No	(1.8×10^{-16})	(4)
		0.143	1.8	–0.08 ± 0.02	No	(1.8×10^{-16})	(4)
AQUA	21	0.088	21	–0.03 ± 0.23	Yes	5.5×10^{-16}	29
F200[b]	125	0.079	16	–0.04 ± 0.03	No	(6.1×10^{-16})	(7)
	152.5	0.079	13			(9.0×10^{-16})	(7)
	180	0.079	10			(13×10^{-16})	(7)

[a] using data generated by HSDM; refers to $MC\text{-}LR_{eq}$

[b] minimum, average and maximum particle diameter were considered for this carbon

[c] whenever Boyd plot does not cross the origin, the D_i value (from Eq. (2)) is presented between brackets since it was obtained out of the model's range of applicability; the same applies to D_i error

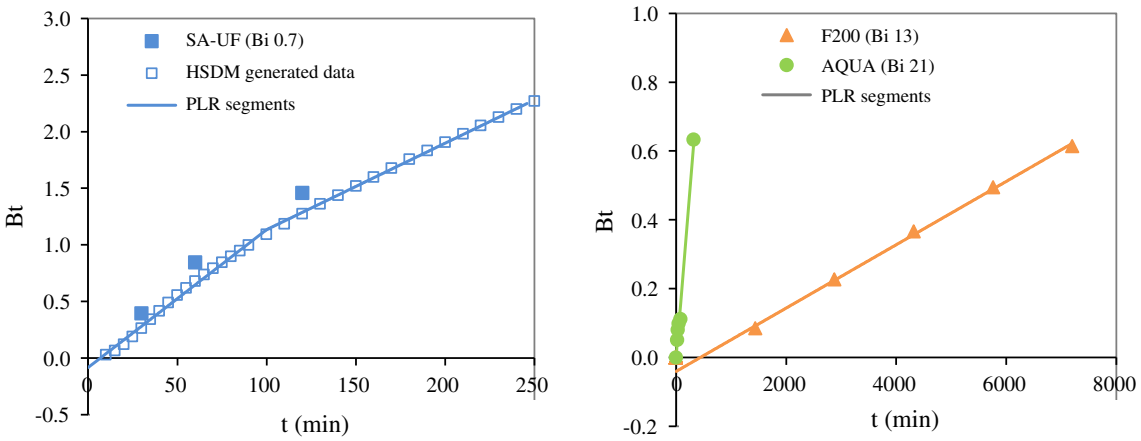

Fig. 4 Boyd plots for MC-LR adsorption onto SA-UF, AQUA and F200 carbons

The good agreement between the HSDM fittings and the experimental data shows that this model can successfully describe the adsorption of MC-LR for the different carbons and initial concentrations studied (Fig. 3).

Taking into account the Biot criteria and for the studied conditions, MC-LR adsorption seems to be controlled by both film transfer and intraparticle diffusion for AQUA and F200, as Biot numbers (Table 5) varied between 15 and 21 (Sect. 2.3; Traegner and Suidan 1989; Roy et al. 1993; Prasad and Srivastava 2009). Concerning fine PAC SA-UF, although Bi values are not $\ll 1$, they are close to 1 and one order of magnitude below those of the previous carbons, which points to a stronger relevance of film transfer.

4.2 Boyd's model results

The equilibrium concentrations (q_e) were estimated by the Freundlich isotherm equation in combination with simple

Table 7 Boyd's model generated results of MC-LR adsorption onto SA-UF and F200 carbons in the 10–100 Biot range

Carbon	d_p (μm)	k_f (m/s)	HSDM D_s (m^2/s)	Results produced using HSDM generated data					
				Bi	C_0 (mg/L)	Bt vs. t intercept	Bt vs. t crosses origin?	Boyd D_i (m^2/s)	D_i error (%)
SA-UF	6	11×10^{-6}	1.0×10^{-16}	10	2.24	0.00 ± 0.01	Yes	1.1×10^{-16}	1
				100	89	0.000 ± 0.001	Yes	1.0×10^{-16}	0.2
F200	152.5	2.0×10^{-6}	4.7×10^{-16}	50	0.529	0.004 ± 0.009	Yes	5.4×10^{-16}	4
				100	1.357	0.003 ± 0.007	Yes	5.1×10^{-16}	3

mass balance. Then, for each kinetic data, F(t) was calculated as q(t)/qe (Eq. 1) and Bt was obtained by applying Eq. (3) if $F(t) > 0.85$ or Eq. (4) if $F(t) \leq 0.85$.

As previously referred (Sect. 2.1), Malash and Khaiary's PLR method was used for defining, on a sound statistical basis, the number and location of breakpoints on Boyd's plots. As the experimental data for the SA-UF carbon were insufficient for PLR application, the HSDM model was used to generate data for this carbon. For AQUA and F200 carbons the PLR method was directly applied. When linearity was found and the plot crossed the origin, D_i was calculated from Eq. (2). Results of the Boyd's model for the three studied carbons, and the associated Biot numbers, are presented in Table 6 and Fig. 4. The D_i errors were calculated for a confidence interval of 95 %.

AQUA Boyd plot produces a straight line (with no breakpoints) passing through the origin. F200 Boyd plot also shows a linear trend (with no breakpoints), although it does not cross the origin. SA-UF Boyd plot shows two linear segments (one breakpoint) and does not intercept the origin. According to Boyd's criterion (El-Khaiary and Malash 2011; Sharma and Das 2012) it can be concluded that, in the studied conditions, intraparticle diffusion was the rate-controlling step for MC-LR adsorption onto AQUA carbon whereas film-diffusion or a combination of both was the rate-limiting step for the remaining carbons. From these results and those obtained with the HSDM and Biot number (Sect. 4.1), it seems that the rate controlling steps are film transfer for SA-UF adsorption, intraparticle diffusion for AQUA and both external and internal transfer for F200.

Boyd's model allows calculating the effective diffusion coefficient (D_i), provided the Boyd plot passes through the origin, which happened only for AQUA carbon. In such case, and considering the associated error, the D_i estimated for MC-LR adsorption was $3.9 \times 10^{-16} - 7.1 \times 10^{-16}$ m^2/s (Table 6), which reasonably agrees with the D_s coefficient obtained with the HSDM, $1.8 \times 10^{-16} - 5.0 \times 10^{-16}$ m^2/s (Table 5) (20 % overlapping of the overall variation range).

The D_i values for SA-UF and F200 carbons are displayed in Table 6 between brackets for highlighting the associated reservations, since they refer to Boyd's plots that do not cross the origin, i.e. to conditions in which Boyd's model is out of its application range for estimating D_i. Actually, in such cases, the diffusion coefficients obtained using the Boyd's model (D_i in Table 6) differ from those obtained with the HSDM (D_s in Table 5), an aspect to be further explored in the next section for a higher range of Bi values.

4.3 Boyd's model analysis for higher Bi values

The HSDM was used to generate Bt vs t data for Bi values of 10 and 100 for SA-UF PAC, and for Bi 50 and 100 for F200 GAC (Table 7). The PLR method was applied to these data and the linear segments obtained are represented in Fig. 5. The Boyd's coefficients (Bt vs t intercept, Di and Di error) are shown in Table 7.

All Boyd plots generated present linear trends crossing the origin. Hence, the diffusion coefficient, D_i, may be calculated. Table 6 shows that, for the simulated conditions, D_i and D_s results are very similar. Analyzing all the Bi values and the diffusion coefficients (Tables 5–7), it may be concluded that when the Boyd plot does not intercept the origin, D_i (estimated by Boyd's model) and D_s (estimated by HSDM) significantly differ, whereas they are reasonably consistent when the Boyd plot crosses the origin. Moreover, as the Bi number increases, the effective diffusion coefficient from Boyd's model decreases and converges to the surface diffusion coefficient from HSDM.

With respect to the rate-limiting step approach, both Biot and Boyd's criteria indicate intraparticle diffusion for SA-UF and F200. The limit above which intraparticle diffusion dominates depends on the carbon: for instance, it must be between 1.8 and 10 for SA-UF, below 21 for AQUA and between 16 and 50 for F200.

The rate limiting step determines the practical options to improve adsorption. When film diffusion is limiting the adsorption, one should improve mixing/turbulence. If intraparticle is the limiting step, finer carbon particles should be used.

5 Conclusions

A comparison was made between the homogeneous surface diffusion model and Boyd's model, namely the model's

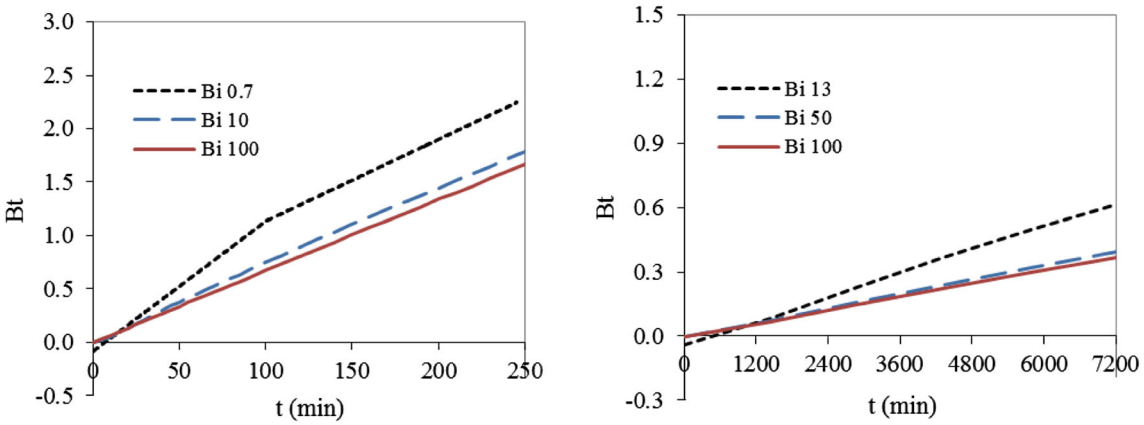

Fig. 5 PLR segments of the Boyd plots for SA-UF (Bi 0.7, 10 and 100) and F200 (Bi 13, 50 and 100)

applicability to establish the adsorption rate-controlling step and to estimate the intraparticle diffusion coefficients. The microcystins adsorption onto three commercial activated carbons used in drinking water treatment was investigated under a wide range of Biot values, i.e. under external and internal diffusion controlled regimes or a combination of both.

Relevant conclusions of this work are

- HSDM was used for the three carbons and achieved very good fittings.
- The Bi limit that establishes the dominance of internal diffusion was found to be dependent on the carbon. Lower Bi limits were observed for carbons with smaller particle diameter.
- When the Boyd plot intercepts the origin, the effective diffusion coefficient estimated by Boyd's model is similar to the surface diffusion coefficient determined from HSDM; when the Boyd's plot does not cross the origin, HSDM must be used to estimate the diffusion coefficient, a crucial parameter for the successful application of adsorption.

Acknowledgments The research leading to these results has received funding from Águas do Algarve, SA (Portugal) and the European Union Seventh Framework Programme (FP7/2007–2013) under grant agreement no. 265122. Rui M.C. Viegas acknowledges the Portuguese Science and Technology Foundation (FCT) for the research grant SFRH/BPD/91875/2012. The authors acknowledge Jussi Meriluoto from Åbo Akademi University (Turku, Finland) for providing the pure MC-LR and the MC-extracts. This publication reflects only the authors' views and the European Union is not liable for any use that may be made of the information contained therein.

References

Baup, S., Jaffre, C., Wolbert, D., Laplanche, A.: Adsorption of pesticides onto granular activated carbon: determination of surface diffusivities using simple batch experiments. Adsorption **6**, 219–228 (2000)

Boschi, C., Maldonado, H., Ly, M., Guibal, E.: Cd(II) biosorption using Lessonia kelps. J. Colloid Interface Sci. **357**, 487–496 (2011)

Boyd, G., Adamson, A., Myers, L.: The exchange adsorption of ions from aqueous solutions by organic zeolites II Kinetics. J. Am. Chem. Soc. **69**, 2836–2844 (1947)

Campinas, M., Rosa, M.J.: The ionic strength effect on microcystin and natural organic matter surrogate adsorption onto PAC. J. Colloid Interface Sci. **299**, 520–529 (2006)

Campinas, M., Viegas, R.M.C., Rosa, M.J.: Modelling and understanding the competitive adsorption of microcystins and tannic acid. Water Res. **47**, 5690–5699 (2013)

Castillejos, E., Rodríguez-Ramos, I., Soria Sánchez, M., Muñoz, V., Guerrero-Ruiz, A.: Phenol adsorption from water solutions over microporous and mesoporous carbon surfaces: a real time kinetic study. Adsorption **17**, 483–488 (2011)

Choy, K.K.H., Porter, J.F., McKay, G.: Film—pore diffusion models—analytical and numerical solutions. Chem. Eng. Sci. **59**, 501–512 (2004)

Cook, D., Newcombe, G.: Comparison and modelling of the adsorption of two microcystin analogues onto powdered activated carbon. Environ. Technol. **29**, 525–534 (2008)

Costa, H.C.R.: Activated carbon adsorption of cyanotoxins from natural waters, PhD thesis in Environmental Sciences and Technologies, Algarve University, Faro, Portugal (2010)

El-Khaiary, M.I., Malash, G.F.: Common data analysis errors in batch adsorption studies. Hydrometallurgy **105**, 314–320 (2011)

Erosa, M.S.D., Medina, T.I.S., Mendoza, R.N., Rodriguez, M.A., Guibal, E.: Cadmium sorption on chitosan sorbents: kinetic and equilibrium studies. Hydrometallurgy **61**, 157–167 (2001)

Ho, Y.S., Mckay, G.: A comparison of chemisorption kinetic models applied to pollutant removal on various sorbents. Trans. Inst. Chem. Eng. **76**, 332–340 (1998)

Li, Q., Snoeyink, V., Mariñas, B., Campos, C.: Elucidating competitive adsorption mechanism of atrazine and NOM using model compounds. Water Res. **37**, 773–784 (2003)

Malash, G.F., El-Khaiary, M.I.: Piecewise linear regression: a statistical method for the analysis of experimental adsorption data by the intraparticle-diffusion models. Chem. Eng. J. **163**, 256–263 (2010)

Marczewski, A.W., Deryło-Marczewska, A., Słota, A.: Adsorption and desorption kinetics of benzene derivatives on mesoporous carbons. Adsorption **19**, 391–406 (2013)

Mathews, A.P., Weber, W.J.J.: Effects of external mass transfer and intraparticle diffusion on adsorption rates in slurry reactors. AIChE Symp. Ser. **166**, 91–107 (1976)

Ocampo-Pérez, R., Abdel Daiem, M.M., Rivera-Utrilla, J., Méndez-Díaz, J., Sánchez-Polo, M.: Modeling adsorption rate of organic micropollutants present in landfill leachates onto granular activated carbon. J. Colloid Interface Sci. **385**, 174–182 (2012)

Ocampo-Pérez, R., Leyva-Ramos, R., Sanchez-Polo, M., Rivera-Utrilla, J.: Role of pore volume and surface diffusion in the adsorption of aromatic compounds on activated carbon. Adsorption **19**, 945–957 (2013)

Prasad, R.K., Srivastava, S.N.: Sorption of distillery spent wash onto fly ash: kinetics and mass transfer studies. Chem. Eng. J. **146**, 90–97 (2009)

Qiu, H., Lu, L.V., Pan, B.C., Zhang, Q.J., Zhang, W.M., Zhang, Q.X.: Critical review in adsorption kinetic models. J. Zhejiang Univ. Sci. A **10**, 716–724 (2009)

Reichenberg, D.: Properties of ion-exchange resins in relation to their structure. III. Kinetics of exchange. J. Am. Chem. Soc. **75**, 589–597 (1953)

Roy, D., Wang, G.-T., Adrian, D.D.: A simplified solution technique for carbon adsorption model. Water Res. **27**, 1033–1040 (1993)

Sathishkumar, M., Pavagadhi, S., Vijayaraghavan, K., Balasubramanian, R., Ong, S.: Experimental studies on removal of microcystin-LR by peat. J. Hazar. Mater. **184**, 417–424 (2010)

Sharma, P., Das, M.R.: Removal of a cationic dye from aqueous solution using graphene oxide nanosheets: investigation of adsorption parameters. J. Chem. Eng. Data **58**, 151–158 (2012)

Sivonen, K., Jones, G.: Cyanobacterial toxins. In: Chorus, I., Bartram, J. (eds.) WHO—Toxic cyanobacteria in water—a guide to their public health consequences, monitoring, and managment, pp. 55–124. E&FN Spon, London (1999)

Traegner, U.K., Suidan, M.T.: Evaluation of surface and film diffusion coefficients for carbon adsorption. Water Res. **23**, 267–273 (1989)

Zhang, Q., Crittenden, J., Hristovski, K., Hand, D., Westerhoff, P.: User-oriented batch reactor solutions to the homogeneous surface diffusion model for different activated carbon dosages. Water Res. **43**, 1859–1866 (2009)

Zhang, H., Zhu, G., Jia, X., Ding, Y., Zhang, M., Gao, Q., Hu, C., Xu, S.: Removal of microcystin-LR from drinking water using a bamboo-based charcoal adsorbent modified with chitosan. J. Environ. Sci. **23**, 1983–1988 (2011)